Dimerization structures of metallic and semiconducting fullerene tubules

Kikuo Harigaya*
Fundamental Physics Section, Physical Science Division, Electrotechnical Laboratory, Umezono 1-1-4, Tsukuba, Ibaraki 305, Japan
and Department of Physics, University of Sheffield, Sheffield S3 7RH, United Kingdom

Mitsutaka Fujita
Institute of Materials Science, University of Tsukuba, Tsukuba, Ibaraki 305, Japan
(Received 12 October 1992)

Possible dimerization patterns and electronic structures in fullerene tubules considered as one-dimensional π-conjugated systems are studied with the extended Su-Schrieffer-Heeger model. We assume various lattice geometries, including chiral and achiral tubules. The model is solved for the case of half-filled π-electron states. (1) When the undimerized systems do not have a gap, the Kekulé structures are prone to occur. The energy gap is of the order of the room temperature and metallic properties are expected to appear. (2) If the undimerized systems have a large gap ($\sim$ 1 eV), the most stable structures are the chainlike distortions where the direction of the arranged *trans*-polyacetylene chains is almost along the tubular axis. The electronic structures are semiconductors due to the large gap.

I. INTRODUCTION

Recently, a new form of carbon, "fullerene tubules," has been synthesized.[1,2] A tubule has the structure like a cylinder made from a graphite sheet. Usually, tubules are observed in multilayered structures. Several tubules interpenetrated. The distance between nearest tubular sheets is about 0.34 nm and is near to that of the separation between the layers in the graphite. The typical diameter of the tubules is of the order of 1 nm. The maximum length of the tubules is more than 1 μm. Thus, a tubule can be regarded as a new class of one-dimensional materials.

The electronical properties have been theoretically calculated.[3-7] A tubule can show metallic or semiconductorlike properties, depending upon its geometry and diameter.[4-6] In these studies,[4-6] all of the carbon atoms have been assumed to be equivalent. All the bonds with the equivalent geometry have identical length. The possibility of bond alternation patterns (namely dimerization) has been considered briefly with reference to the in-plane[3,7] and out-of-plane[5] dimerization. It was concluded that the strength of the dimerization might be quite small even if it occurs.

It is, however, well known that the one-dimensional systems are unstable with respect to Peierls distortions if a weak electron-phonon interaction is present. Dimerization will appear in fullerene tubules due to the Peierls instabilities. The dimerization patterns will depend on the structure of the tubules. The possible patterns have not been investigated in detail in the previous works.[3,5,7] Therefore, it would be interesting to study what patterns can appear when we regard tubules as quasi-one-dimensional π-conjugated systems.[8]

In this paper, we extend the Su-Schrieffer-Heeger (SSH) model[9] of conjugated polymers to the honeycomb network system in order to apply to fullerene tubules. The electronic properties and the possible dimerization patterns are analyzed using the finite-size-scaling method.[7] We obtain the "Kekulé structure" for the metallic tubules, and the "chainlike distortion" for the semiconducting tubules as the most stable state. The Kekulé structure is a network of hexagons with the alternating short and long bonds like in the classical benzene molecule. The chainlike distortion is a pattern where *trans*-polyacetylene chains are connected by long bonds in the direction perpendicular to the chains. The Kekulé or chainlike patterns will be important as fluctuations, even though the amplitude of dimerizations is of the same order as that of the fluctuations and therefore it is difficult to observe the static distortions.

In the next section, we explain our model and ideas of the investigation. In Sec. III, the Kekulé structures in the metallic tubules are reported. In Sec. IV, the chainlike distortions in the semiconducting tubules are discussed. We close this paper with several remarks in Sec. V.

II. MODEL AND FORMALISM

We use the extended SSH Hamiltonian[7,9] for investigation of dimerization patterns. The model is

$$H = \sum_{\langle i,j\rangle,\sigma} (-t_0 + \alpha y_{i,j})(c^{\dagger}_{i,\sigma} c_{j,\sigma} + \text{H.c.}) + \frac{K}{2} \sum_{\langle i,j\rangle} y^2_{i,j}, \tag{1}$$

where $c_{i,\sigma}$ is an annihilation operator of a π electron, quantity t_0 is the hopping integral of the ideal undimerized system, α is the electron-phonon coupling, $y_{i,j}$ indicates the bond variable which measures the length change

of the bond between the ith and jth sites from that of the undimerized system, and the sum is taken over nearest-neighbor pairs $\langle ij \rangle$. The second term is the elastic energy of the lattice, and the quantity K is the spring constant. This model is numerically solved by the iteration method used in the previous studies[7,10] under the assumption of the adiabatic approximation.

We shall look at the dependences on parameters. The value of $t_0 = 2.5$ eV is taken from that of graphite and polyacetylene, and has been used in the previous papers.[7,10] We fix the spring constant $K = 49.7$ eV/Å^2 and change the coupling constant α, so that the dimensionless electron-phonon coupling $\lambda \equiv 2\pi\alpha^2/\pi K t_0$, analogous to that in BCS superconductivity, has various values. Although the realistic value would be about 0.2 as we have used for C_{60}, C_{70}, and tubules in the previous papers,[7,10] we scan the parameter space up to $\lambda = 1.4$ to see the relative stability among possible solutions.

In Fig. 1, we show a set of vectors which specify the tubules on the honeycomb lattice. The lattice points in the honeycomb lattice are labeled by the vector $(m, n) \equiv m\mathbf{a} + n\mathbf{b}$, where $\mathbf{a}$ and $\mathbf{b}$ are the unit vectors. Any structures of tubules can be produced by connecting the two parallel lines which pass (0,0) and (m, n) and are perpendicular to the vector (m, n). Hereafter, we use this vector (m, n) to specify the tubules. When the electron-phonon coupling does not exist, i.e., $\lambda = 0$, the electronic state of the tubule is classified into metal or semiconductor depending on the vector. When the origin of the honeycomb lattice pattern is superposed with one of the open circles to make a tubule, the metallic properties will be expected because of the presence of the Fermi surface. This case corresponds to the vectors where $m - n$ is a multiple of 3. If the origin is superposed with the filled circles, there remains a large gap of the order of 1 eV. The system will be a semiconductor. The similar properties regarding the metallic and semiconducting behaviors have been discussed in several recent papers.[4–6]

When there is a nonzero electron-phonon coupling, several kinds of bond-ordered configurations can be expected. One of them in the two-dimensional graphite plane is the Kekulé structure. The pattern is superposed with the honeycomb lattice in Fig. 1. The short and long bonds are indicated by the thick and normal lines, respectively. This pattern is commensurate with the lattice structure for the tubules when $m-n$ is multiples of 3 in the vector (m, n), because the Kekulé structure is the three sublattice system. Therefore, we expect that the Kekulé structure is one of the candidates for the most stable solutions. For other tubules, the Kekulé pattern misfits the boundary condition of the tubule due to the structural origin. In contrast, one-dimensional chainlike patterns, where *trans*-polyacetylene chains are connected by the long bonds in the transverse direction, can be realized for any set of (m, n).

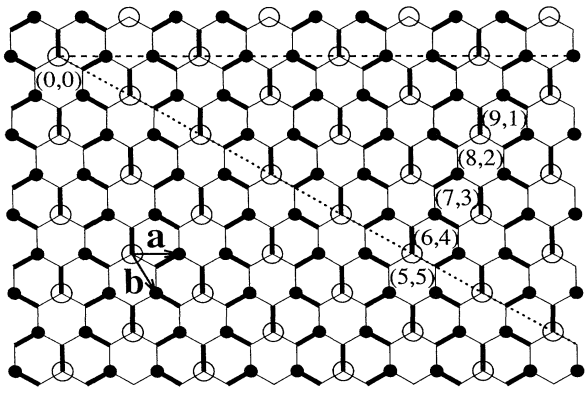

FIG. 1. Possible way of making chiral and achiral tubules. The open and closed circles indicate the metallic and semiconductoring behaviors of the undimerized system, respectively. The Kekulé structure is superposed on the honeycomb lattice pattern. The heavy lines indicate the short bonds.

We shall explain our strategy of the investigation. When the origin $(0, 0)$ is combined with $(5, 5)$, we obtain an achiral tubule which has a reflection plane. In Ref. 5, this tubule has been named as the "armchair" fiber. Both the Kekulé and chainlike patterns are the candidates for the stationary solutions. Furthermore, when we make the tubule $(6, 4)$, we cut all the rings of ten carbons in tubule $(5, 5)$ and connect the neighboring rings to each other. The tubule loses the reflection symmetry and becomes chiral. In this tubule, the Kekulé pattern misfits the structure and the chainlike distortions will be realized. If we connect next-nearest-neighboring rings, we obtain the tubule $(7, 3)$. The tubule becomes more chiral. There will be chainlike patterns. For the tubule (8,2), both the Kekulé and chainlike structures become possible again. Repeating the above procedure further, we obtain the achiral "zigzag" fiber at (10,0).[5] We pursue changes in dimerization patterns and electronic energy levels, starting from the tubule $(5, 5)$.

III. KEKULÉ STRUCTURES IN METALLIC TUBULES

When Kekulé structures are commensurate with the honeycomb lattice pattern, we actually obtain such patterns as one of stationary solutions. These are for the cases of the tubules (5,5) and (8,2). We mainly report the results of the tubule (5,5) with brief comments for the tubule (8,2). The system size N is varied within $300 \leq N \leq 600$. The periodic boundary condition is applied for the direction of the tubular axis.

For the tubule (5,5), we consider several dimerization patterns, which are indicated in Fig. 2. In Figs. 2(a) and 2(b), the lattice patterns are Kekulé type. In Fig. 2(b), the positions of the short and long bonds are reversed from those in Fig. 2(a). Figure 2(b) contains hexagons, where all the sides are short bonds. Such short bonds are not the double bonds of ordinary meaning, so they are denoted by the dashed lines. Figures 2(c) and 2(d) show the chainlike patterns. There are several directions of the chains. For the tubule (5,5), we only consider the directions of chainlike patterns shown in the figure, because numerical data for the set of the bond lengths and energy levels for patterns with the other directions are the same. There are other possible patterns where the signs of the bond variables become opposite from those in Figs.

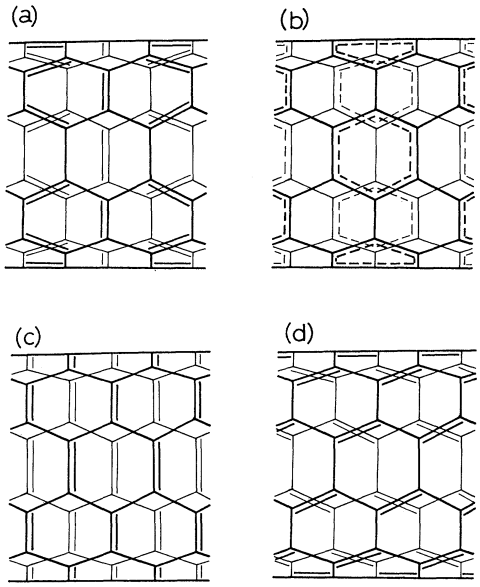

FIG. 2. Dimerization patterns of the stationary solutions for the tubule (5,5). Front and back views are shown by the normal and thin lines, respectively. See the text for notations.

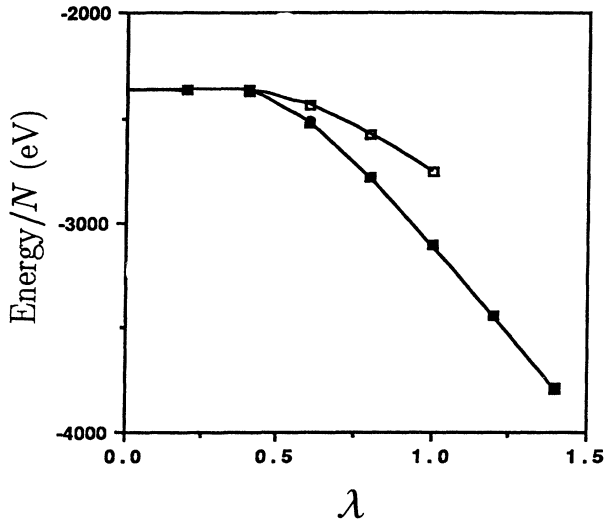

FIG. 3. Total energy per site vs λ for the tubule (5,5). The system size is $N = 600$. The closed squares are for the patterns (a), (c), and (d) (the plots are not discernible), while the open squares are for (b) in Fig. 2.

2(c) and 2(d). We have tried to obtain such kinds of solutions by changing initial bond variables appropriately. But, we have never obtained them, possibly because the energy might be much larger or unstable. Thus, we shall report the results for the patterns depicted in Fig. 2. We note that the Kekulé pattern of Fig. 2(a) has been discussed in Refs. 3 and 7 but chainlike patterns have not been considered previously. We have analyzed possible patterns more extensively.

First, the total energies of the above patterns are shown against the coupling λ in Fig. 3. The number of carbons is $N = 600$. The energy decreases almost linearly for the strong coupling $\lambda \sim 1$. The energies of the patterns (a), (c), and (d) seem to be almost the same. However, there are differences larger than 1 eV. This is clearly reflected to values of the energy gap, which will be discussed in association with Fig. 4. The energy of pattern (b) is much larger than that of the others. Thus, the pattern with the reversed alternation of the short and long bonds is energetically unfavorable.

The energy gap is plotted against λ for each pattern in Fig. 4. Pattern (a) has the widest gap for $0 < \lambda < 0.8$. This indicates that the Kekulé structure is most stable for the realistic parameter $\lambda \sim 0.2$. The other patterns are the metastable states. When $1.0 < \lambda < 1.4$, pattern (d) becomes most stable. The energy gap $E_g = 6t_0 = 15.0$ eV is realized for all patterns from (a) to (d). This is due to the fact that the order parameters are extraordinarily large at the strong coupling.

Hereafter, we shall discuss properties of the system with $\lambda = 0.2$. The data for $300 \leq N \leq 600$ are used for the analysis. This region of N might yield sufficient data for estimation of electronic and lattice structures. We shall concentrate upon properties of the stable solutions, i.e., the Kekulé structure of Fig. 2(a).

In Fig. 5, the total energy per site is plotted against $1/N$. Data points can be fitted well by the parabola curve. The extrapolated value to infinite N is -3.9341 eV. This value does not change if we fit data by a third- or fourth-order polynomial.

Figure 6 shows the energy gap E_g of the tubule (5,5). The gap varies linearly as a function of $1/N$ due to the one-dimensional nature. When $N \sim 100$, E_g is of the order of 1 eV. When $N \sim 500$, it becomes of the order of 0.1 eV. The extrapolated value at $N \to \infty$ is 4.39×10^{-3} eV. This is apparently lower than room temperature. In

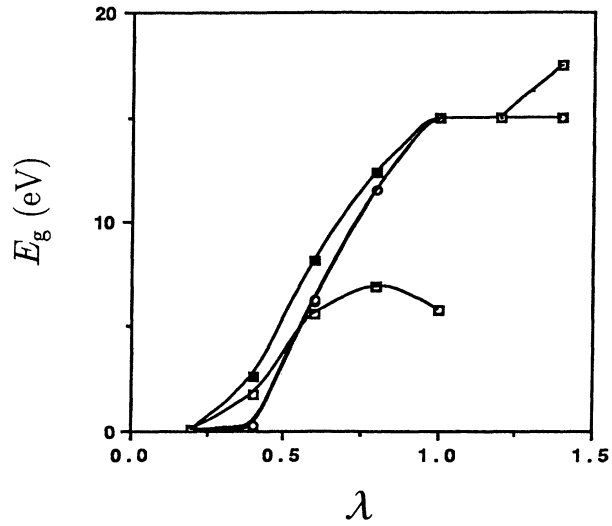

FIG. 4. Energy gap vs λ for the tubule (5,5) with $N = 600$. The closed and open squares are for the patterns (a) and (b), respectively. The closed and open circles are for (c) and (d).

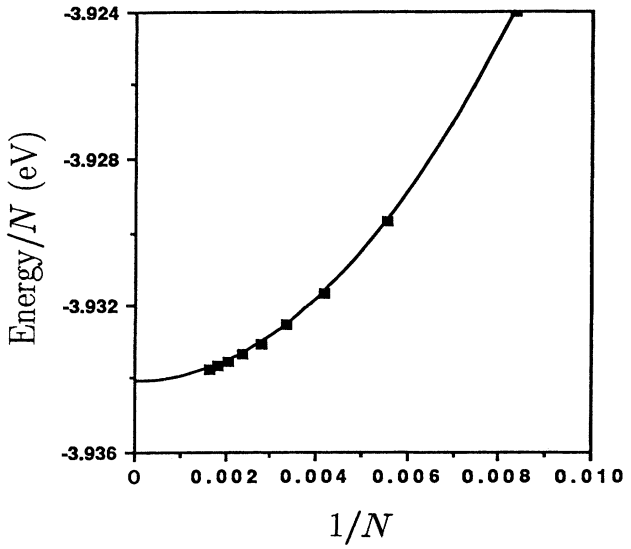

FIG. 5. The $1/N$ dependence of the energy per site of the tubule (5,5).

addition, we should pay attention to the thermal fluctuation of phonons. Thus, we can expect nearly metallic behaviors even at low temperatures.

Figure 7(a) shows the average of the absolute values of the bond variables, $\langle|y_{i,j}|\rangle$. This measures the strength of dimerizations. The value of C_{60} is 2.22×10^{-2} Å. The average $\langle|y_{i,j}|\rangle$ decreases linearly as a function of $1/N$ due to the one dimensionality. The extrapolated value at $N \rightarrow \infty$ is 7.52×10^{-4} Å. This is more than one order of magnitude smaller than the observed value in C_{60} (Ref. 10) and polyacetylene.[8,9] Figure 7(c) displays the $1/N$ dependence of the bond variables with the labels of the bonds in Fig. 7(b). The length difference between the

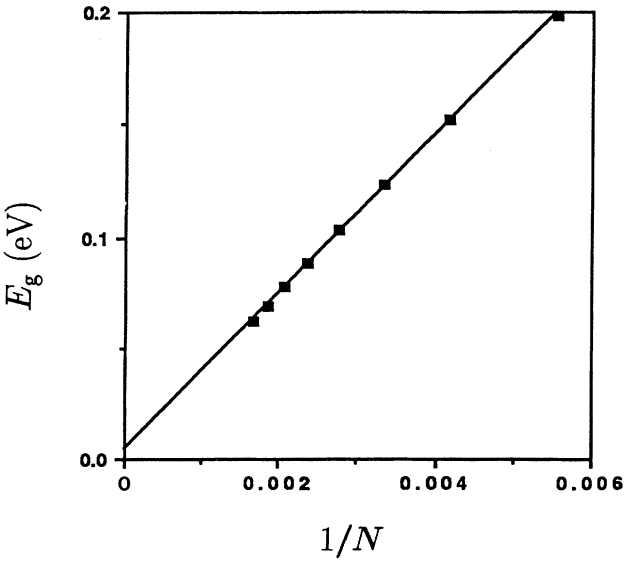

FIG. 6. The $1/N$ dependence of the energy gap E_g of the tubule (5,5).

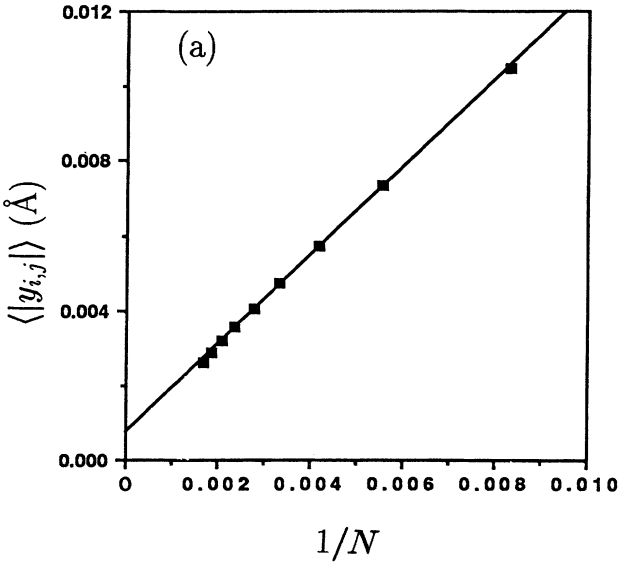

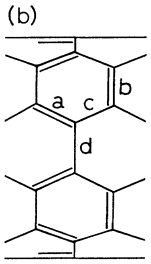

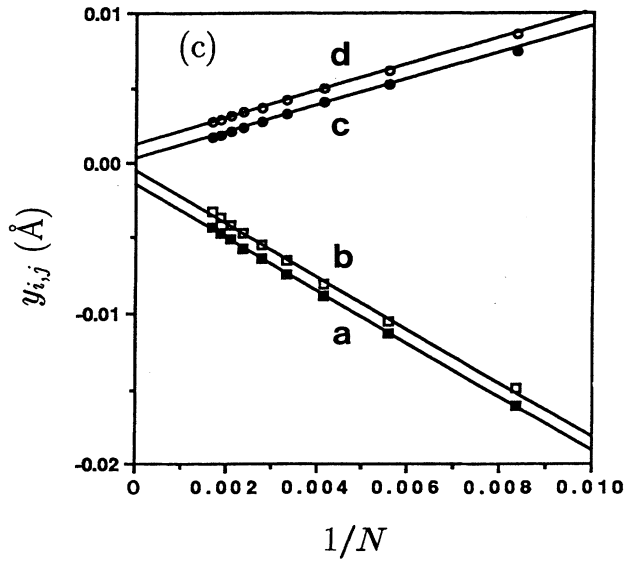

FIG. 7. The $1/N$ dependence of the bond variables of the tubule (5,5). The averaged bond variable $\langle|y_{i,j}|\rangle$ is shown in (a). The labels of bonds are shown in (b). (c) shows the variations of each bond length.

longest and shortest bonds of C_{60} is 0.05 Å in the present parameters.[10] When $N \sim 500$, the value becomes about one-tenth of it. This would be smaller than the maximum value (about 0.01 Å) of the dimerization strength observable in experiments. In the narrowest tubules actually present, the maximum length is about 1000 times that of the tubule diameter.[1] Such tubules can be regarded as infinitely long. The extrapolated value of the length difference is 2.64×10^{-3} Å. It has been discussed that the widths of the fluctuations of the bond lengths are of similar magnitudes (of the order of 10^{-2} Å) in conjugated polymers, graphite plane, and C_{60}.[3,11] The large fluctuations would make the observation of the pattern difficult. Even though the pattern could not be observed directly, the Kekulé-type fluctuations might survive thermal fluctuations if we look at, for example, the correlation functions among lengths of different bonds.

We have also calculated the tubule (8,2). We have obtained the Kekulé structure as the most stable solution again. The energy gap E_g and the magnitudes of the bond variables are not so much different from those of the tubule (5,5), quantitatively. The number of carbons arranged around the axis is ten for both tubules. This indicates that the electronic and lattice properties are mainly determined by the diameter of tubules. They do not sensitively depend on whether the tubule is chiral or not.

In the previous paper,[7] we have looked at the variation of electronic and lattice structures from C_{60} and C_{70} to an infinitely long tubule (5,5). Ten more carbons have been inserted successively for the systematic investigation of changes in C_{60}, C_{70}, C_{80}, and so on. The linear $1/N$ dependence is similarly found in the data of E_g and the bond variables. We have concluded the Kekulé pattern with small dimerization strengths in the lattice structure, too.

IV. CHAINLIKE DISTORTIONS IN SEMICONDUCTING TUBULES

In this section, we discuss the tubules, (6,4) and (7,3). In these tubules, the Kekulé pattern is automatically excluded owing to the boundary condition. We have obtained only the solutions where the *trans*-polyacetylene chains are arranged along almost the tubular axis. Solutions where chains are oriented in other directions are not obtained. The pattern in the tubule (6,4) is shown in Fig. 8. Numerical data are reported for $\lambda = 0.2$.

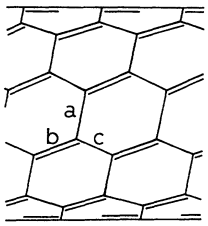

FIG. 8. The dimerization pattern of the stationary solution for the tubule (6,4).

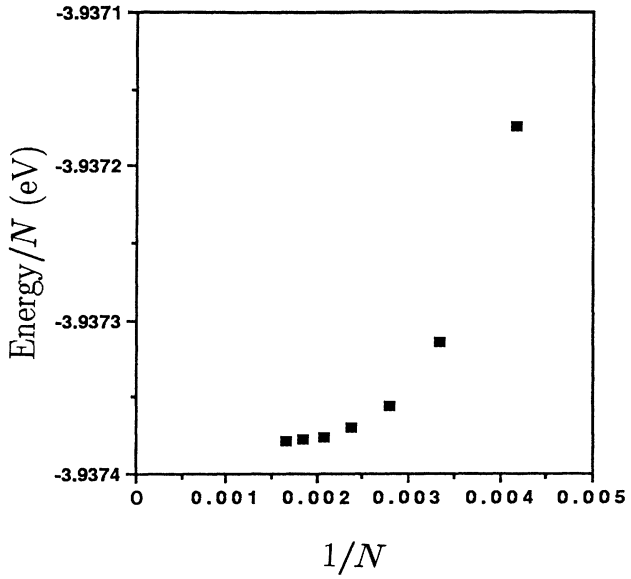

FIG. 9. The $1/N$ dependence of the energy per site of the tubule (6,4).

We plot the energy per site vs $1/N$ in Fig. 9. It seems that the energy stops decreasing at $N \sim 500$. Figure 10 shows E_g of the tubule (6,4) as a function of $1/N$. The energy gap almost saturates at $N \sim 600$. The large gap (~ 1 eV) remains when $N \to \infty$. These saturating properties are due to the fact that there is a wide gap even in the system with $\lambda = 0$. The system is a semiconductor whether there is a dimerization pattern or not.

Figure 11(a) shows the variation of the averaged bond variable. This also saturates at $N \sim 500$. The value at $N \to \infty$ is about 1.1×10^{-3} Å. The dimerization strength is close to that in the nearly metallic tubules.

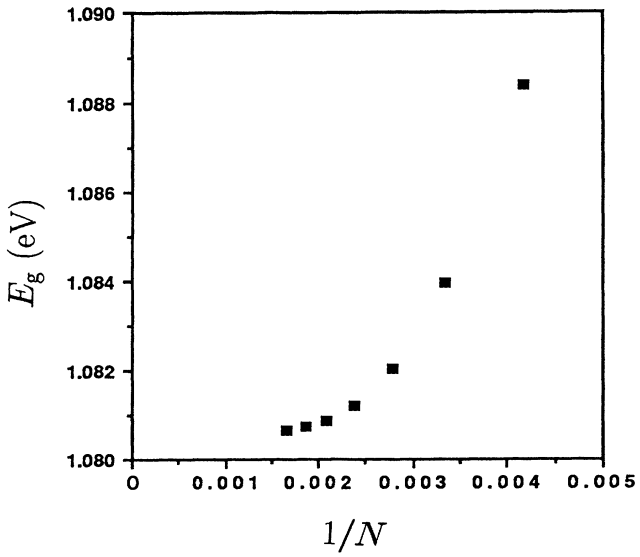

FIG. 10. The $1/N$ dependence of the energy gap E_g of the tubule (6,4).

This does not depend on whether there is a gap or not when $\lambda = 0$. The strength would be determined mainly by the number of carbons which lie perpendicular to the tubule axis. It is ten for all the tubules calculated in this paper. In Fig. 11(b), we show the bond variables against $1/N$. The label of each bond is shown in Fig. 8. The strength of the dimerization is very small: the length difference between the shortest and the longest bonds is about 0.003 Å. This value is of the magnitude similar to that found in Fig. 7(c). The shortest and longest bonds alternate parallel to the tubular axis. The bond order is the strongest in this direction along the "*trans*-polyacetylene" chains. This would reflect the one dimensionality.

For the tubule (7,3), we have obtained the same kind of solutions as the stable solution. The bond alternation pattern is chainlike. The energy gap and the strength of the dimerization do not change so much from those in Figs. 10 and 11.

V. CONCLUDING REMARKS

We have investigated the tubules where ten carbons are arranged in the direction perpendicular to the tubular axis. We have obtained the similar strength of dimerizations for the Kekulé structure and the chainlike distortion. The Kekulé pattern is the most stable for the metallic tubules, while the chainlike pattern is realized for the semiconducting tubules. The strength of the dimerizations is about one order smaller than the experimentally accessible magnitude. Therefore, it would be difficult to observe directly the bond alternation patterns in the very long tubules. However, the fluctuations of the phonons from the classical values might show some correlations which reflect the Kekulé or chainlike patterns.

We have estimated the properties of infinitely long tubules by the finite-size-scaling method. Certainly, there would be numerical errors in the extrapolated values. Calculations using the wave-number space would result in more accurate magnitudes. However, the present calculations should be valid enough to estimate the overall magnitudes of the energy gap and the dimerization strength.

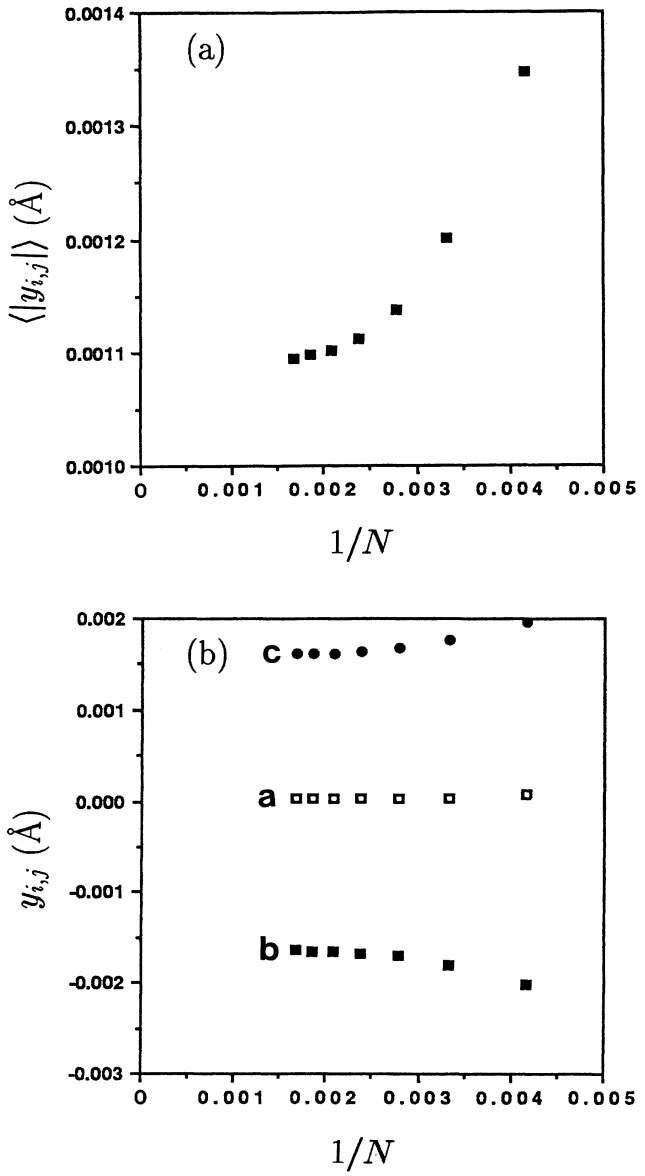

FIG. 11. The $1/N$ dependence of the bond variables of the tubule (6,4). The averaged bond variable $\langle|y_{i,j}|\rangle$ is shown in (a). The labels of bonds are shown in Fig. 8. (b) shows the variations of each bond length.

ACKNOWLEDGMENTS

The author (K.H.) acknowledges useful discussion with Dr. K. Yamaji, Dr. S. Abe, Dr. Y. Asai, and Dr. T. Miyazaki. He also acknowledges the hospitality of the Department of Physics, University of Sheffield, United Kingdom, and financial support for the stay. A part of this work was done while one of the author (M.F.) was staying at the Department of Physics, Massachusetts Institute of Technology. He is grateful for the fruitful collaboration with Professor Mildred S. Dresselhaus, Professor Gene Dresselhaus, and Dr. R. Saito. Numerical calculations have been performed on FACOM M-780/20 and M-1800/30 of the Research Information Processing System, Agency of Industrial Science and Technology, Japan.

*Electronic addresses: harigaya@etl.go.jp and e9118@jpnaist.bitnet

[1]S. Iijima, Nature (London) **354**, 56 (1991); T. W. Ebbesen and P. M. Ajayan, *ibid.* **358**, 220 (1992).

[2]M. Endo, H. Fujiwara, and E. Fukunaga (unpublished).

[3]J. W. Mintmire, B. I. Dunlap, and C. T. White, Phys. Rev. Lett. **68**, 631 (1992).

[4]N. Hamada, S. Sawada, and A. Oshiyama, Phys. Rev. Lett.

68, 1579 (1992).
[5]R. Saito, M. Fujita, G. Dresselhaus, and M. Dresselhaus, Phys. Rev. B **46**, 1804 (1992).
[6]K. Tanaka, M. Okada, K. Okahara, and T. Yamabe, Chem. Phys. Lett. **193**, 101 (1992).
[7]K. Harigaya, Phys. Rev. B **45**, 12 071 (1992).
[8]A. J. Heeger, S. Kivelson, J. R. Schrieffer, and W. P. Su, Rev. Mod. Phys. **60**, 781 (1988).
[9]W. P. Su, J. R. Schrieffer, and A. J. Heeger, Phys. Rev. B **22**, 2099 (1980).
[10]K. Harigaya, Phys. Rev. B **45**, 13 676 (1992).
[11]R. H. McKenzie and J. W. Wilkins, Phys. Rev. Lett. **69**, 1085 (1992).